Paper 55

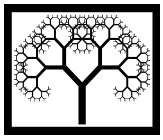


Proceedings of the Eleventh International Conference
on Computational Structures Technology,
B.H.V. Topping, (Editor),
Civil-Comp Press, Stirlingshire, Scotland

# A Mixed Mode Cohesive Law for Z-Pinned Composite Delamination

**H. Cui[1,2], S. Koussios[1], Y.-L. Li[2] and A. Beukers[1]**
**[1] Faculty of Aerospace Engineering**
**Delft University of Technology, the Netherlands**
**[2] School of Aeronautics**
**Northwestern Polytechnical University, P.R. China**

## Abstract

A new methodology for modeling Z-pin reinforcement in composite laminates is presented, in which continuum cohesive elements are used to represent the Z-pins. A coupled cohesive zone model is developed to incorporate both the interlaminar failure and the failure of Z-pins. The standard mode I/II delamination toughness tests of Z-pinned composite laminates and the Z-pinned composite T-joints subject to bending load were analysed. Comparison between the numerical simulation and the experimental results approved the applicability and validity of the present model. The modeling methodology allows for convenient implementation and is flexible enough to account for different Z-pin densities and distributions. The successful application of the methodology to other reinforcements has also been demonstrated.

**Keywords:** Z-pin, mixed mode, composites, cohesive law, T-joint, stitch, delamination, DCB, ENF.

# 1 Introduction

Carbon fiber reinforced composite laminates are extensively used in many structural applications as they profit from their high strength/weight ratio. Delamination is the dominating failure mode for composite laminates due to their weak performance in the through-the-thickness direction. A popular solution for this problem is the Z-pinning method, which is based on inserting carbon or metallic rods in the thickness direction of laminates [1]. Experiments showed that Z-pins can significantly increase the fracture toughness of laminates [2, 3]. Z-pinning is regarded to be less effective at resisting the crack initiation, but sufficiently effective at resisting the propagation of long cracks [4].

Accompanying the increasing application of Z-pins, modeling methods have to be introduced to analyze and facilitate the design of Z-pin reinforced composite structures. The finite element method provides a very general and flexible modeling

tool; therefore several calculations have been carried out to analyze the failure of Z-pinned composite laminates.

One possible approach to model the Z-pin response is averaging the Z-pin bridging forces over the whole interfacial area, namely, the equivalent distributed cohesive model. The mode I double cantilever beam (DCB) test was analyzed by Robinson and Das [5] and Dantuluri et al. [6] using this approach. It was shown to yield good results when the distance between these Z-pins is small enough; however, its accuracy drops significantly when the space between adjacent Z-pins is increased.

The other feasible approach is modeling individual Z-pins as discrete nonlinear springs, these 2-D spring elements were connected between nodes located on the delamination surfaces. The mode I/II delamination toughness of Z-pinned laminates has been analyzed by Yan et al. [7, 8], the mixed mode delamination has also been simulated with this methods by Zhang and her cooperators [9, 10]. Recently, this method was used for the numerical analysis of composite T-joints subject to shear, bending and pull-off load [11, 12]. However, the engineering application of this method suffers from several drawbacks in practice: (1) the spring element is defined by two initially coincident nodes on both sides of the potential delamination surface, which means the overall mesh and node coordinates have to be painstakingly designed, making it difficult and time-consuming to account for an arbitrary Z-pin density and distribution; (2) representing the bridging effect of individual Z-pins by single-node force is a serious potential source of numerical error [6], which may preclude the convergence of computation(and the results become strongly mesh dependent); (3) only the axial stress can be undertaken by 2-D spring elements, the mode I bridging force that arrests the crack opening and the mode II bridging force that arrests the crack sliding are just the components of the axial force in orthogonal directions. Correspondingly, the mode I/II bridging forces follow exactly the same damage evolution law in 2-D spring element model, while there actually are some differences between experiments and numerical simulations. On the other hand, Zhang [13] presented a new modeling strategy that uses a cohesive zone model (CZM) for predicting delamination growth of Z-pinned laminates, while only mode I delamination was taken into account.

The main object of this paper is to introduce a new modeling methodology for analyzing Z-pinned composite laminates, and verify the feasibility and validity of the new model. A coupled CZM is presented here to incorporate both the interlaminar failure and the failure of the Z-pins. Cohesive elements of different constitutive behaviors were involved: a traditional bilinear cohesive law was used to simulate normal delamination of laminates, a novel mixed mode cohesive law was developed to represent the failure response of Z-pins. The bridging response of the Z-pins was obtained by a micro-mechanics model developed by the author [14].

# 2 Modelling methodology

## 2.1 Single Z-pin model

The developed numerical model for analyzing the bridging mechanisms of Z-pinning in composite laminates is briefly introduced here. The failure process of the

Z-pin during single or mixed mode delamination is very complicated, consisting of debonding and frictional sliding at the interface between the Z-pin and surrounding matrix, resin deformation, Z-pin splitting and rupturing. As shown in Figure 1, the splitting and rupturing within the Z-pin were simulated by CZM. The interfacial contact between the Z-pin and matrix was assumed to be initially bonded, followed by debonding and frictional sliding. The Z-pin was loaded via a prescribed displacement of the upper laminate, and the mode mix ratio was defined as the scale of its displacements along *X* and *Z* coordinates.

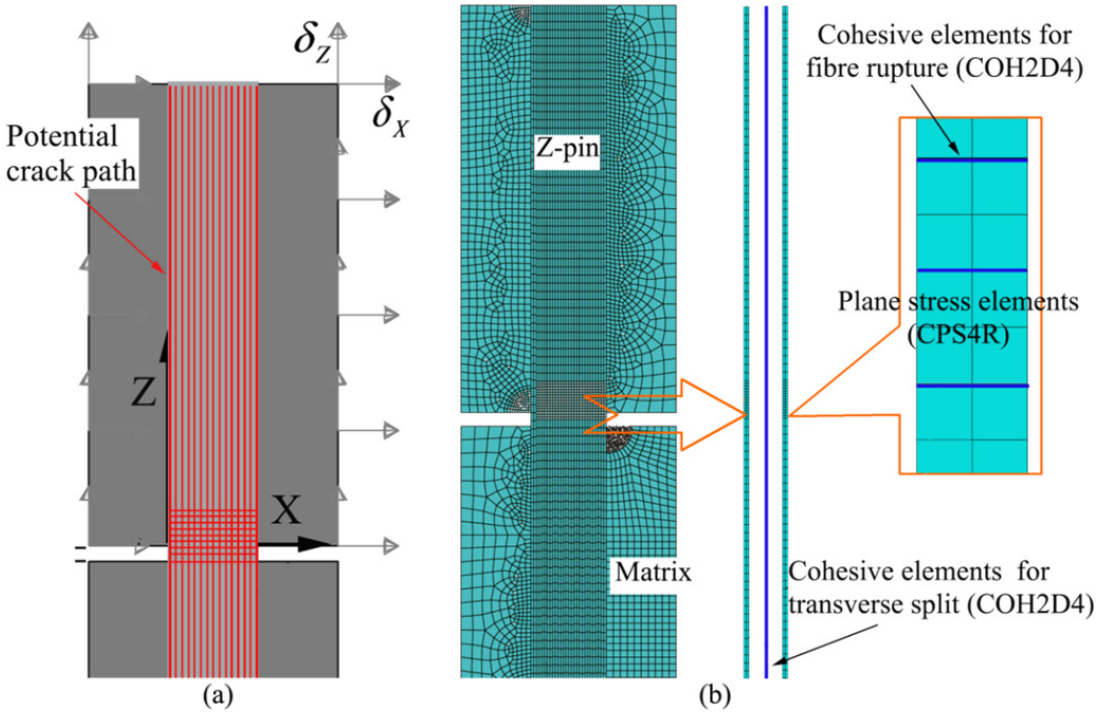


Figure 1. Single Z-pin model: (a) geometry and loading condition; (b) finite element mesh

The Z-pin investigated here is made with T300/BMI, with a diameter of 0.28 [mm]. The material properties used for the single Z-pin model are shown in Table 1. The bridging response of the Z-pin in mixed mode delamination was predicted using the single Z-pin model. The bridging force vs. displacement in pull-off and shear directions can be obtained, the data shown in Figure 2 has been reduced, in order to be used as input parameters in the next section to obtain the mixed mode cohesive law**.**

| $E_{11}$[GPa] | $E_{22}$[GPa] | $v_{12}$ | $G_{12}$[GPa] | $\sigma_l$[MPa] | $\sigma_t$[MPa] | $\tau_s$[MPa] |
|---|---|---|---|---|---|---|
| 123 | 7.31 | 0.25 | 5 | 1200 | 80 | 101 |

Table 1. Mechanical properties of T300/BMI lamina

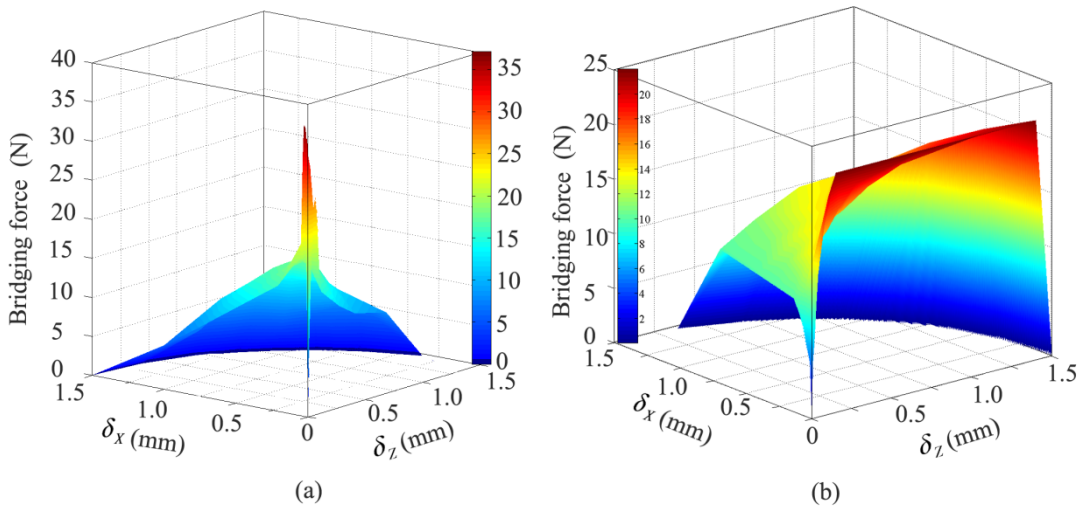


Figure 2. Mixed mode bridging force: (a) mode I component; (b) mode II component

## 2.2 Mixed mode cohesive law for Z-pins

CZM on the base of traction laws are well suited for the analysis of delamination in composite structures [15], in which the cohesive law is defined in terms of traction versus separation (displacement of cohesive element). The cohesive element usually is linear elastic at its initial stage; the process of degradation begins when the stresses and/or strains satisfy specified damage initiation criteria [16]. The maximum nominal stress criterion was utilized here:

$$\max\left\{\frac{\langle t_n\rangle}{t_n^o},\frac{t_s}{t_s^o}\right\}=1 \tag{1}$$

Where the $\langle\ \rangle$ Means $\langle a\rangle=(a+|a|)/2$; and $t_n^o$, $t_s^o$ are the mode I and II interlaminar strength values.

Once the corresponding initiation criterion is reached, the material stiffness is degraded; this is governed by the damage evolution law. A scalar damage variable, *D*, represents the overall damage in the material; it initially has a value of 0. It monotonically evolves from 0 to 1 upon further loading after the initiation of damage while the degraded *K* stiffness is determined as:

$$K=K_0\left(1-D\right) \tag{2}$$

where $K_0$ is the initial stiffness. In this paper, the damage evolution law is extracted from the predicted mixed mode bridging forces, and the scalar damage variable is calculated as a function of the displacement:

$$D(\delta)=1-\frac{(\sigma/\delta)}{K_0} \tag{3}$$

Two different damage evolution laws, respectively corresponding to the mode I and II bridging response were obtained as shown in Fig. 3. These relations will be used as inputs for the finite element model, presented in the next section.

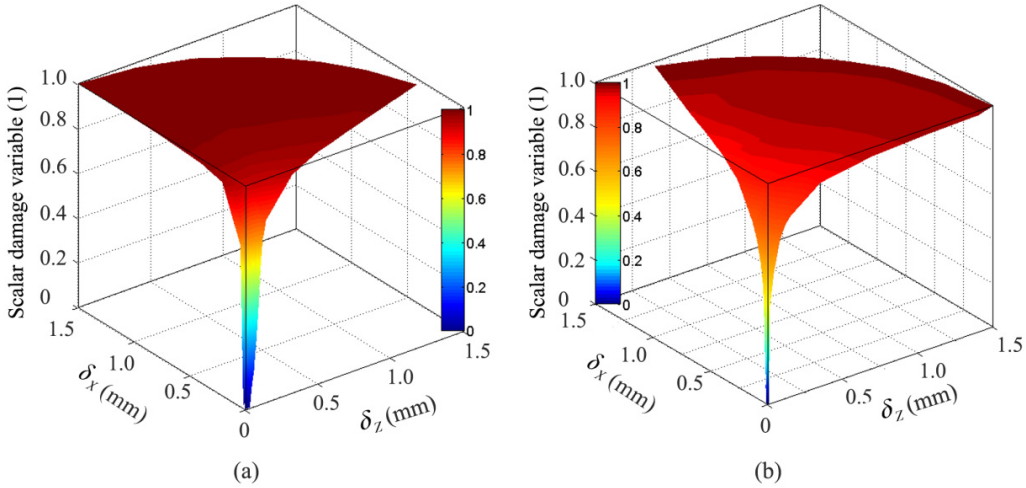


Figure 3. The scalar damage variable as function of mixed mode displacement: (a) mode I response; (b) mode II response

## 2.3 Z-pin mesh generation

Figure 4 presents the modeling strategy for Z-pins in composite laminates. The cohesive elements used for simulating the laminate delamination were defined with two different cohesive laws: the mixed mode Z-pin bridging response (that has been introduced in the previous section) and the simple bilinear cohesive law representing the failure of the unreinforced laminate [17]. Both surfaces of the cohesive elements were connected with the adjacent laminate surface via the "Tie" constraint, available in the commercial software "ABAQUS". The displacement and stress were continuous at the interface while the element density and node coordinates can be different for the cohesive layer and the laminates. Hence, the mesh of the cohesive layer can be generated independently, making it easy to account for different Z-pin distributions without changing the mesh of the laminates. The cohesive stress is calculated by averaging the overall Z-pin bridging force over the whole cohesive element; consequently, the surface areas of the cohesive elements are not necessary to be identical at the Z-pin cross section.

# 3 DCB and ENF simulation

## 3.1 DCB and ENF model

In this paper, the DCB test for measuring the mode I fracture toughness, and the End Notched Flexure (ENF) test for measuring the mode II fracture toughness have been simulated for both unpinned and Z-pinned composite laminates. The specimen geometry and material data were taken from [18], and their configuration is shown in Figure 5.

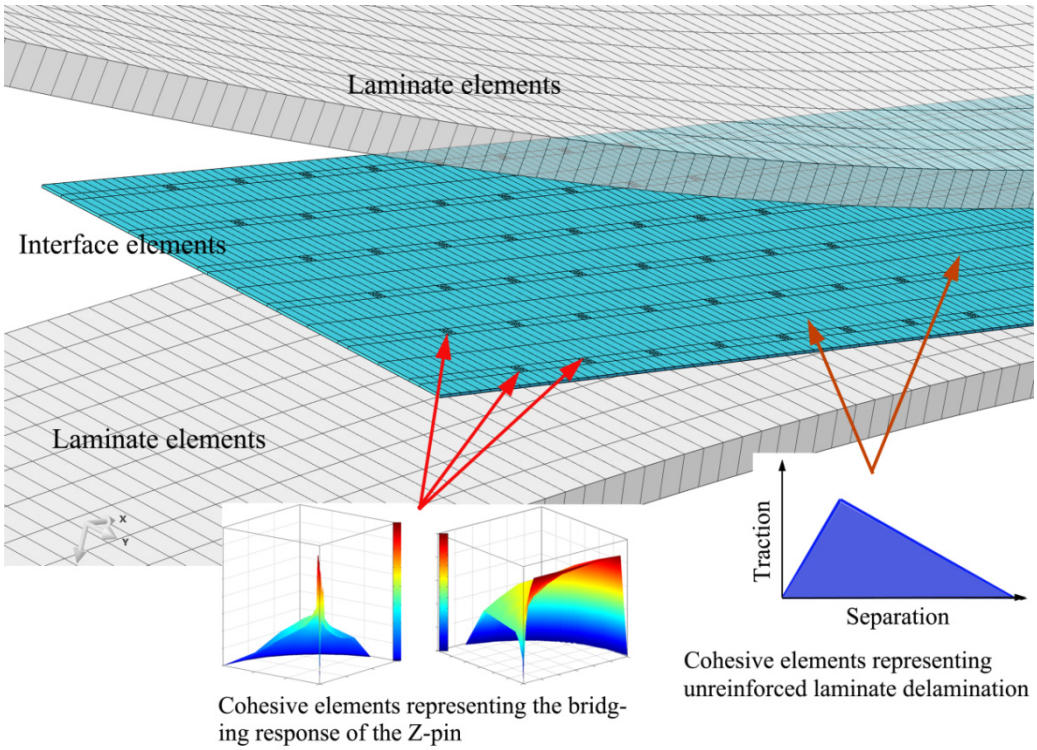


Figure 4. Mesh generation for Z-pinned laminates

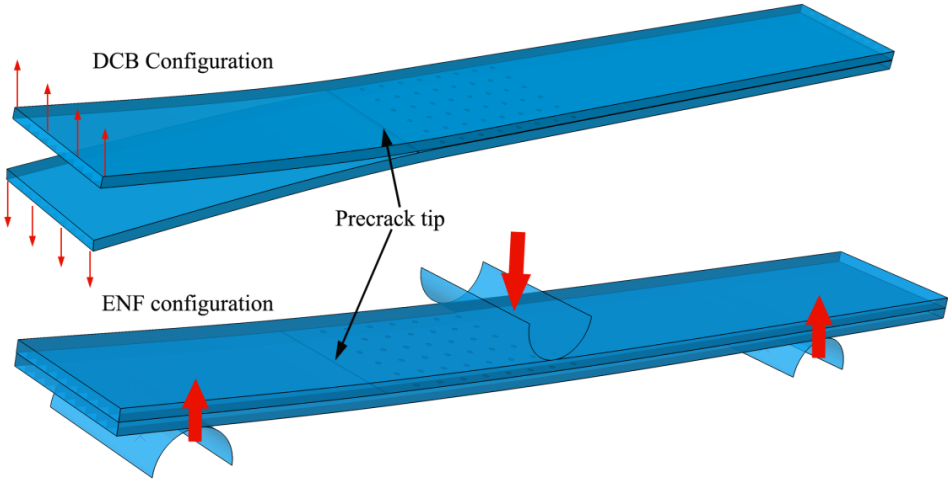


Figure 5. Z-pinned DCB and ENF configurations

## 3.2 Results and discussion

The failure process of Z-pinned the DCB specimen is shown in Figure 6, it clearly indicates that the Z-pins were still bridging the laminates even when the crack tip propagated through them for quite a long distance. The predicted load-displacement

curves of both DCB and ENF specimens are plotted in Figure 7. The unpinned and Z-pinned DCB simulations agree with the experiments reasonably well, the damage initiation load and maximum load values from simulation coincide with the ones obtained from the experiments. For the ENF simulation, the damage initiation load was predicted accurately with the present model, while deviation between experiments and simulations came out after damage occurrence as instable crack propagation taking place for the unpinned ENF specimen in the experiments.

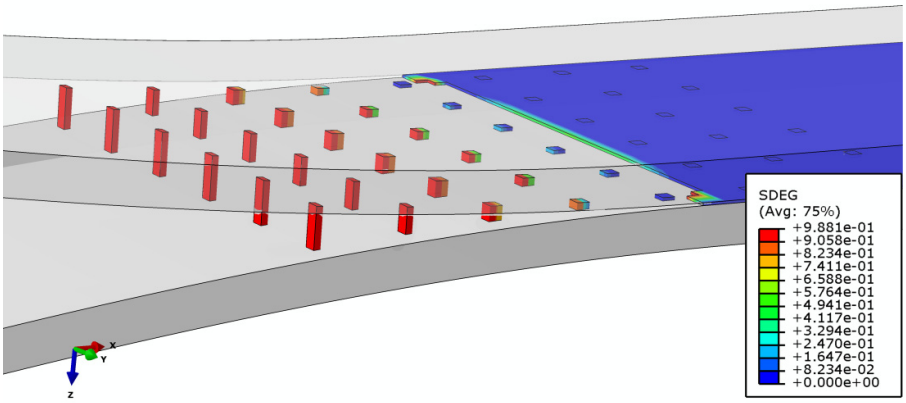


Figure 6. Failure process of Z-pins in DCB specimen

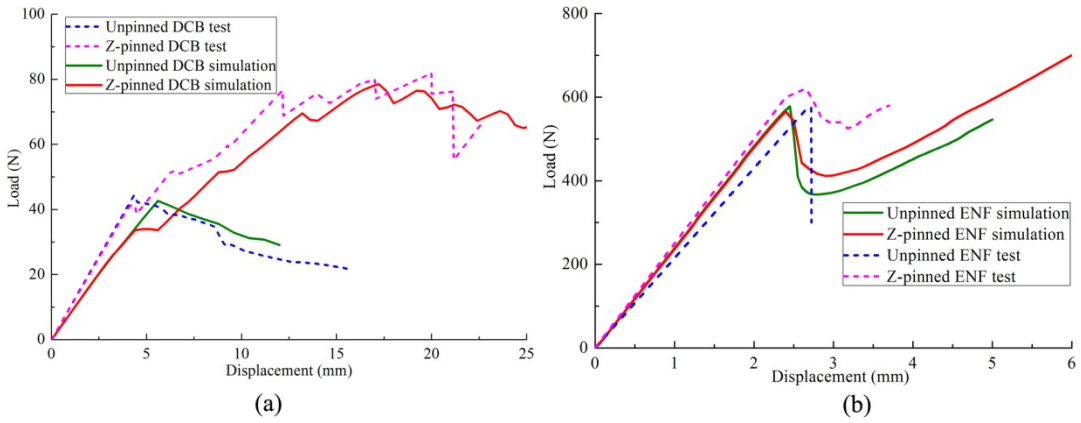


Figure 7. Load-Displacement curves for (a) DCB experiments and simulations; (b) ENF experiments and simulations

# 4 T-joint simulations

## 4.1 T-joint bending test

The composite T-joint is made up of three T700/QY8911 laminates, the material properties of which are shown in Table 2. The stringer and skin are connected by

adhesive at the interface, as shown in Figure 8. The Δ-filler region at the root of the stiffener was filled with unidirectional prepreg tape, and the filler is also connected with the laminates by adhesive film. The specimen was placed on a steel support during the experiment. The load was applied by an indenter with the same width as the specimen; the radius of the indenter nose is 5 mm. It was located 45 mm above the skin-stringer junction. At the end of the specimen, a steel fixture has been mounted for preventing specimen-support separation. The Z-pins were made of T300/BMI with the material properties shown in Table 1, and the pin to pin spacing was 3 [mm].

| $E_{11}$[GPa] | $E_{22}$[GPa] | $v_{12}$ | $G_{12}$[GPa] | $G_{13}$[GPa] | $G_{23}$[GPa] |
|---|---|---|---|---|---|
| 135 | 9.12 | 0.311 | 5.67 | 5 | 5 |

Table 2. T700/QY8911 material properties

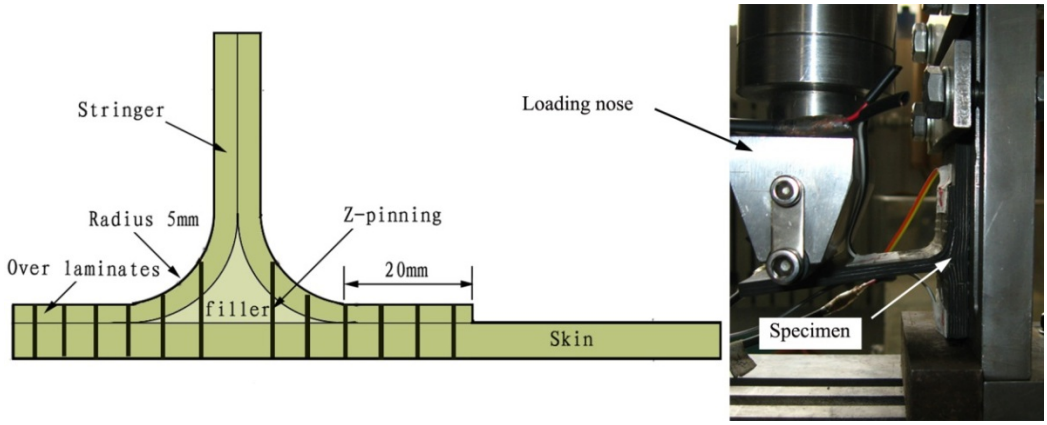


Figure 8. Composite T-joint specimen geometry and test configuration

## 4.2 Finite element model

A finite element model was developed for the T-joint specimen for which the mesh generation strategy is outlined in Section 2.2. The width of the model is equal to the pin to pin spacing, and the Z-pins are located in the mid-width as shown in Figure 9. The laminates were meshed with a quadrilateral continuum shell element (SC8R), for which the reduced integration method with hourglass control was utilized. The 8-node cohesive three-dimensional cohesive element (COH3D8) was used for simulating both the laminate delamination and Z-pin failure process. The interface between the laminates and the filler was modeled by the "cohesive surface" method in ABAQUS, the cohesive law was identical as the one used for simulating the delamination of unreinforced laminates (see Table 3).

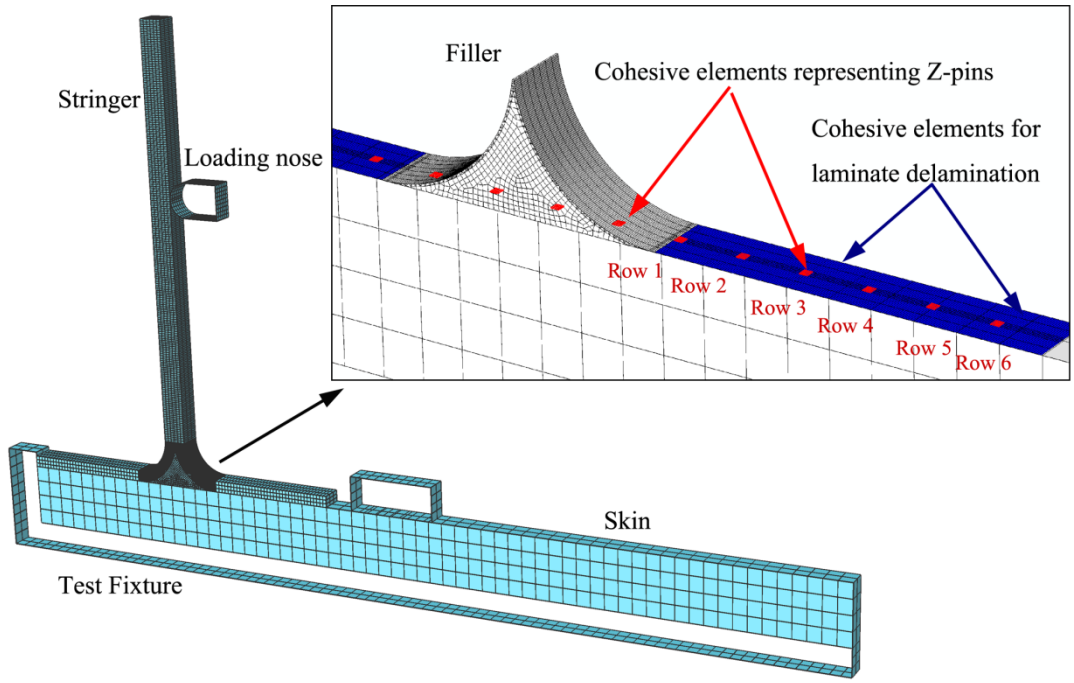


Figure 9. The finite element model of Z-pinned composite T-joint

| $K_n$[MPa/$mm$] | $K_s$[$MPa/mm$] | $t_n^0$ [MPa] | $t_s^0$[MPa] | $G_{IC}$[$N/mm$] | $G_{IC}$[$N/mm$] |
|---|---|---|---|---|---|
| 3e6 | 1.15e6 | 25 | 15 | 0.252 | 0.665 |

Table 3. Mechanical properties of cohesive elements for analyzing unreinforced laminates

## 4.3 Results and discussion

Figure 10 presents the failure process of T-joint specimens with and without Z-pin reinforcements, subject to bending load. The load-displacement curve is almost linear at the initial part of the curve until the onset of cracking. At the instance of damage initiation, a sharp drop of the load-displacement curve can be observed. The cracking occurred first at the interface between the filler and the laminates because of the high geometric stress concentration here and the large mismatch in the elastic modulus.

As the nose displacement was increasing, the crack propagated into the interface between the skin and stringer followed by cracking on the other side of the filler. However, the load of Z-pinned specimen increased again with reduced slope, and exceeded thereby the value of the initial damage load. The damage initiation loads from both experiments and simulations coincide with each other, and the maximum load of Z-pinned specimen was predicted by the present model reasonably well.

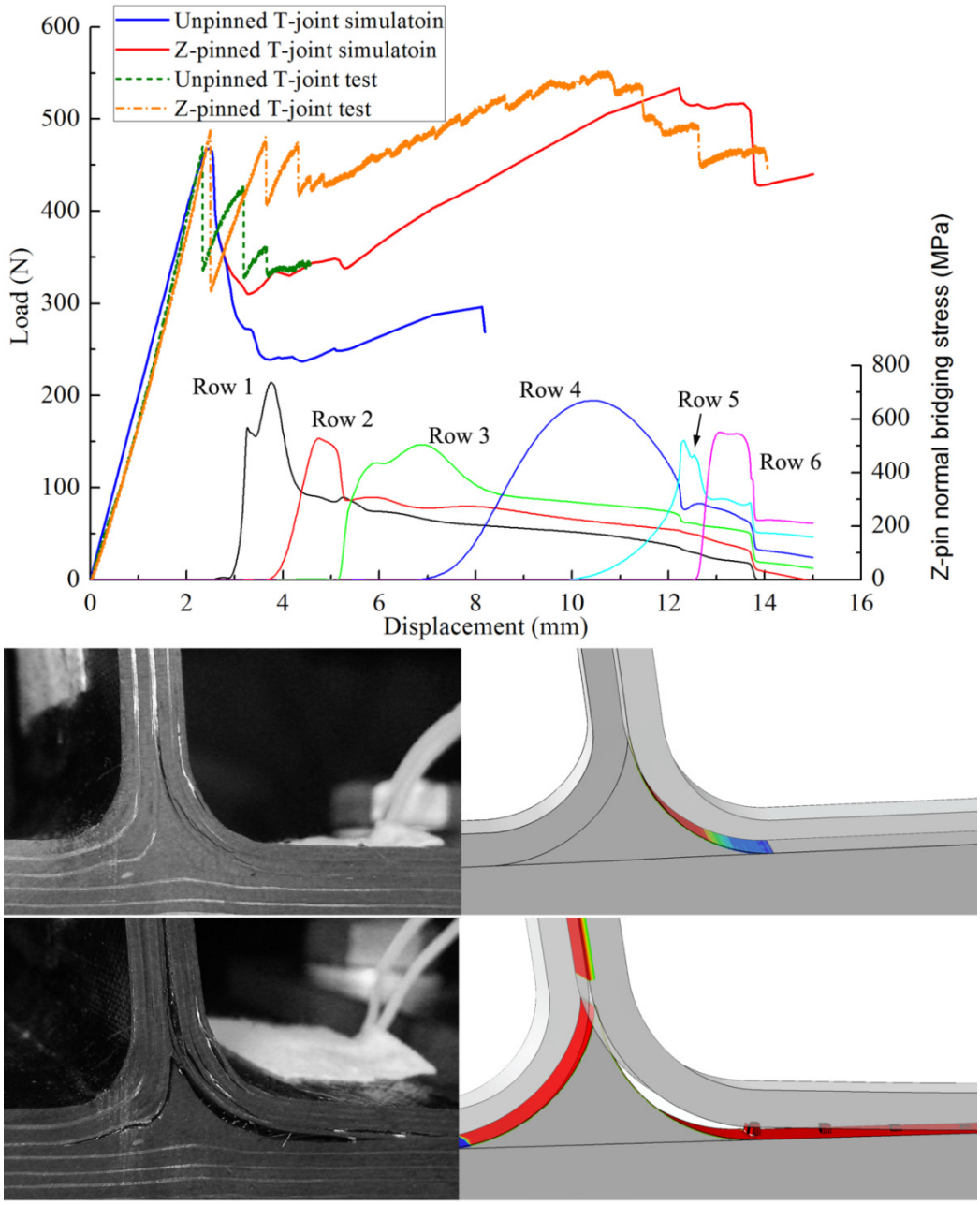


Figure 10. Failure process of T-joints subject to bending load

The mode I bridging stress history of Z-pins during the failure process is also shown in Fig. 10. The rows of Z-pins were numbered by their distance from the filler, and the "Row 1" Z-pin is closest to the edge of the filler (see Figure 9.). As the crack tip passed through, each row of Z-pins came sequentially into play which resulted in the higher loading capacity of Z-pinned T-joints as compared to that of of unpinned ones after the crack initiation.

# 5 Simulation for stitching

The present modeling methodology for Z-pinned structures has been validated in various applications in the previous sections: standard test methods such and DCB and ENF, and T-joints are frequently being used in composites. In this section, the applicability of the methodology was extended to the analysis of composite laminates reinforced by other kinds of reinforcement, like stitching. The bending failure of stitched T-joint is thus analyzed. The geometry and laminate information of stitched T-joints were identical as for the Z-pinned ones (Figure 8.). The stitch fibers were Kevlar 964D yarns with a stitch-to-stitch spacing of 5 [mm].

The bridging model for stitch reinforcements is derived from the experimental observation of the failure mechanisms of stitch yarns [19, 20]. The bridging force of stitch fibers increases at first instance monotonously with the crack opening displacement, and is ended with a sudden drop caused by the rupture of stitch fibers. Only a small friction force is active during the pull-out phases of ruptured thread. In this paper, the maximum stitching bridging force is calculated by the tensile strength, multiplied by the stitch yarn cross section area. The resulting bridging model used for numerical analysis is presented in Figure 11.

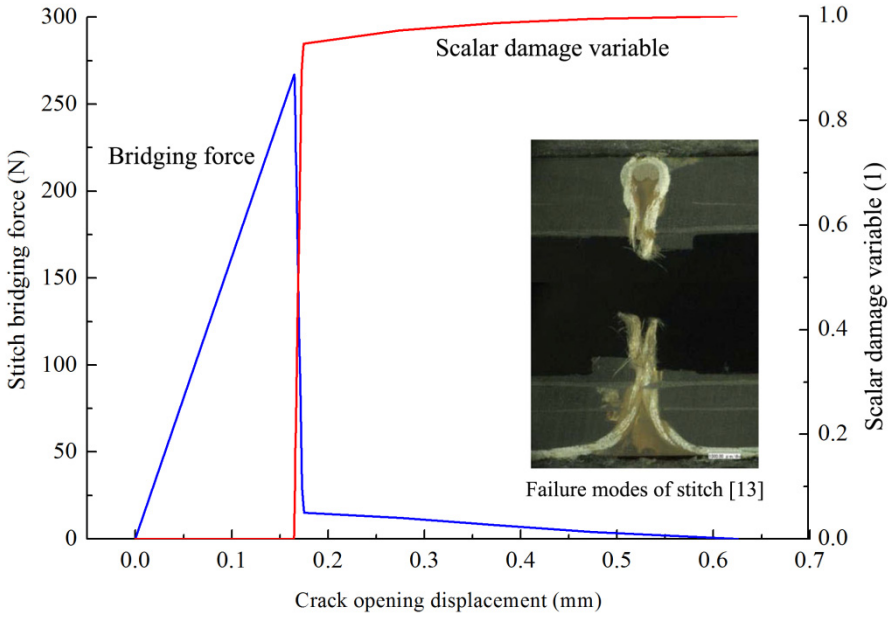


Figure 11. Bridging model of the stitch

The predicted load-displacement curves from the present model are shown in Figure 12. The zigzag" behavior of the load curves of stitched T-joint is more distinct than for the Z-pinned ones; this is mainly due to the fact that the stitch row supplies higher bridging force that prevents the crack from opening while the stitch to stitch spacing is bigger when compared with Z-pins. The cohesive stress that represents the stitch bridging effect is also sketched in Figure 12, where the stitch

rows were numbered in a similar way as shown in Figure 9. Good correlation between the failure process of each row of stitching and the "zigzag" on the load curve can be observed. Hence, the present model has demonstrated its applicability in analyzing stitched composite structures.

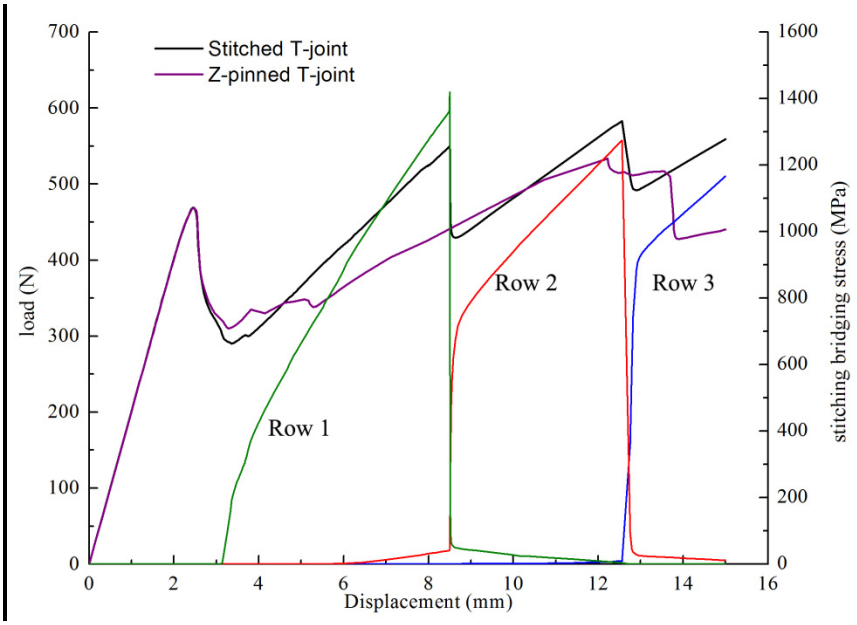


Figure 12. Numerical simulation of stitched T-joint subject to bending load

# 6 Conclusions

In this paper, an improved method is presented, in which Z-pin reinforcement is represented by cohesive elements. The mixed mode cohesive law describing the bridging response of Z-pins was obtained with a meso-scale finite element model. The present method is used for analysing DCB/ENF tests of composite laminates, and the bending failure of Z-pinned composite T-joints. The comparison between experiments and numerical simulation demonstrate the applicability and show the accuracy of this modelling method. The methodology presented here is easy to carry outand is flexible enough for the accounting of different Z-pin configurations and laminate constructions.

Experiments and simulations indicate that Z-pinning may not increase the damage initiation load, while the maximum load of the T-joint was significantly improved. Other through-thickness-reinforcements such as stitching can also be taken into account using the present model, provided that their bridging response during mixed mode delamination is known.

# References


[1] G. Freitas, T. Fusco, T. Campbell, J. Harris, Roesenberg S, "Z-fiber technology and products for enhancing composite design", In: AGQRD conference Proceedings 17-1-8,1996.

[2] G. Freitas, C. Magee, Dardzinski, T. Fusco, "Fiber insertion process for improved damage tolerance in aircraft laminates", J Adv Mater, 25, 36–43, 1994.

[3] K.L. Rugg, B.N.Cox, M. Massabo, "Mixed mode delamination of polymer composite laminates reinforced through the thickness by Z-fibers", Composites Part A, 33, 177-190, 2002.

[4] A.P. Mouritz, "Review of z-pinned composite laminates", Composites: Part A, 38, 2383–2397, 2007.

[5] P. Robinson, S. Das, "Mode I DCB testing of composite laminates reinforced with z-direction pins: a simple model for the investigation of data reduction strategies", Engineering Fracture Mechanics, 71(3), 345–64, 2004.

[6] V. Dantuluri, S. Maiti, P.H. Geubelle, R. Patel, H. Kilic. "Cohesive modeling of delamination in Z-pin reinforced composite laminates". Composites Science and Technology, 67, 616-631, 2007.

[7] W. Yan, H.Y. Liu, Y.W. Mai, "Numerical study on the mode I delamination toughness of z-pinned laminates", Composites Science and Technology, 63, 1481–1493, 2003.

[8] W. Yan, H.Y. Liu, Y.W. Mai. Y. W, "Mode II delamination toughness of z-pinned laminates", Composites Science and Technology, 64, 1937–1945, 2004.

[9] M. Grassi, B.N. Cox, X. Zhang, "Simulation of pin-reinforced single-lap composite joints", Composites Science and Technology, 66, 1623–1638, 2006.

[10] G. Allegri, X. Zhang, "On the delamination and debond suppression in structural joints by Z-fibre pinning", Composites: Part A, 38, 1107–1115, 2007.

[11] J.T. Vazquez, B. Castanie, J.J. Barrau, N. Swiergiel, "Multi-level analysis of low-cost Z-pinned composite joints Part 1: Single Z-pin behavior", Composites: Part A, 42, 2070-2081, 2011.

[12] J.T. Vazquez, B. Castanie, J.J. Barrau, N. Swiergiel, "Multi-level analysis of low-cost Z-pinned composite joints Part 2: Joint behavior", Composites: Part A, 42, 2082-2092, 2011.

[13] F. Bianchi, X. Zhang, "A cohesive zone modelfor predicting delamination suppression in z-pinned laminates, Composites Science and Technology, 71, 1898-1907, 2011.

[14] H. Cui, Y.L. Li, S. Koussios, A. Beukers, "Bridging micromechanics of Z-pin in mixed mode delamination", Composite Structures, 93, 2685-2695, 2011.

[15] R. Borg, L. Nilsson, K. Simonsso, "Simulating DCB, ENF and MMB experiments using shell elements and a cohesive zone model", Composite Science and Technology, 64, 269-278, 2004.

[16] Abaqus 6.11 Analysis User's Manual, 2011

[17] H. Cui, L-Y. Li, S. Koussios, A. Beukers, “Parametric evaluation on the curved part of composites T-joints based on numerical simulation” in “27th international congress of the aeronautical sciences”, Nice, France, 2010.
[18] D.D.R. Cartie, “Effect of Z-fibres on the delamination behavior of Carbon Fibre/Epoxy Laminates”, PhD Thesis, Cranfield University, 2000.
[19] K.T. Tan, N. Watanabe, Y. Iwahori, “Experimental investigation of bridging lae for single stitch fibre using interlaminar tension test”, Composite Structures, 92(6),1399-1409, 2010.
[20] Y. Iwahori, K. Nakane, N. Watanabe. “DCB test simulation of stitched CFRP laminates using interlaminar tension test results”, Composites Science and Technology, 69, 2315–2322, 2009.